

See discussions, stats, and author profiles for this publication at: <https://www.researchgate.net/publication/231667855>

# Molecular Orientation and Electrochemical Stability of Azobenzene Self-Assembled Monolayers on Gold: An In-Situ FTIR Study

ARTICLE *in* LANGMUIR · JULY 2000

Impact Factor: 4.46 · DOI: 10.1021/la000054m

CITATIONS

23

READS

33

5 AUTHORS, INCLUDING:



**Shen Ye**

Hokkaido University

133 PUBLICATIONS 3,874 CITATIONS

SEE PROFILE



**Hao-Li Zhang**

Lanzhou University

200 PUBLICATIONS 3,450 CITATIONS

SEE PROFILE



**Kohei Uosaki**

National Institute for Materials Science

467 PUBLICATIONS 9,073 CITATIONS

SEE PROFILE

# Molecular Orientation and Electrochemical Stability of Azobenzene Self-Assembled Monolayers on Gold: An In-Situ FTIR Study

Hua-Zhong Yu,<sup>\*,†</sup> Shen Ye,<sup>‡</sup> Hao-Li Zhang, Kohei Uosaki,<sup>\*,‡</sup> and Zhong-Fan Liu\*

Center for Nanoscale Science and Technology (CNST), College of Chemistry and Molecular Engineering, Peking University, Beijing 100871, China, and Physical Chemistry Laboratory, Division of Chemistry, Graduate School of Science, Hokkaido University, Sapporo 060, Japan and Department of Chemistry, Acadia University, Wolfville, Nova Scotia B0P 1X0, Canada

Received January 18, 2000. In Final Form: May 4, 2000

The relationship between the physical properties of azobenzene self-assembled monolayers (SAMs) on gold surfaces ( $C_nH_{2n+1}-O-\phi-N=N-\phi-C(O)NHC_mH_{2m}S-Au$ , abbreviated as  $C_nAzoC_mS-Au$ ) and the structural nature of the parent alkanethiol molecules was investigated by electrochemical in-situ Fourier transform infrared reflection/absorption spectroscopy (FTIR–RAS). The  $2H^+$ ,  $2e^-$  redox behavior from azobenzene to hydrazobenzene in  $C_nAzoC_mS-Au$  monolayers was confirmed, as reported in our recent paper (*Langmuir* **1998**, *14*, 619–624). The in-situ spectra showed unambiguously that the molecular orientation and electrochemical stability of azobenzene SAMs are highly related to the structural nature of the azobenzene alkanethiols. In particular, the longer the alkyl chains in the azobenzene alkanethiols, the more stable and closely packed are the monolayers. A potential-induced orientational switching of the terminal ethoxy group was observed for  $C2AzoC4S-Au$ , which is different from the intermolecular hydrogen-bonding “fixed” alkyl chain below the azobenzene moiety.

## 1. Introduction

Recently, we reported the redox behavior of azobenzene self-assembled monolayers (SAMs) on gold ( $C_2H_5-O-\phi-N=N-\phi-C(O)NHC_{10}H_{20}S-Au$ , abbreviated as  $C2AzoC10S-Au$ ) investigated by electrochemical in-situ Fourier transform infrared reflection/absorption spectroscopy (FTIR–RAS).<sup>1</sup> This work as well as the concurrent in-situ FTIR–RAS studies of  $\phi-N=N-\phi-OC_{10}H_{20}S-Au$ ,<sup>2</sup> and the in-situ Raman spectroscopic measurements of  $Fe-\phi-N=N-\phi-C_4H_8S-Au$  ( $Fe = (\eta^5-C_5H_5)Fe(\eta^5-C_5H_4)$ ),<sup>3</sup> elucidated the  $2H^+$ ,  $2e^-$ , reduction/oxidation process of azobenzene to hydrazobenzene in monolayers on gold in contact with aqueous electrolytes. Direct evidence for the unusual redox kinetics, i.e., slower reduction of azobenzene compared to the oxidation of hydrazobenzene in these closely packed monolayers was provided.<sup>1,2</sup> Our interest in the construction and characterization of azobenzene functionalized monolayer systems stems from the unique photochromism and electrochemistry of azobenzene-tethered organic thin films, which impact on the potential applications in areas such as “molecule-based” ultrahigh-density information storage and electronic devices.<sup>4–6</sup> In the past decade, various azobenzene alkanethiols have been shown to form densely packed and highly oriented monolayers on gold surfaces. The electron-transfer process in both aqueous and nonaqueous electrolytes, the photoswitching behavior, and the molecular packing and order

of these azobenzene SAMs on gold have been extensively investigated.<sup>1–3,7–20</sup>

In this paper, we report our extended electrochemical in-situ FTIR–RAS studies of a series of azobenzene SAMs on gold ( $C_nH_{2n+1}-O-\phi-N=N-\phi-C(O)NHC_mH_{2m}S-Au$ , abbreviated as  $C_nAzoC_mS-Au$ , where  $n = 0$  for  $m = 2$ ,  $n = 1$  for  $m = 2$ , and  $n = 2$  for  $m = 4$ ). The variation of the alkyl chains is not as extensive as that involved in our previous studies,<sup>7–11</sup> but the selections are essential and adequate to show the effect of both inner alkyl chain and terminal group on the overall properties of the monolayers. As mentioned above, there have been a few reports involving in-situ spectroscopic studies of azobenzene SAMs,<sup>1–3</sup> but none have dealt with the effect of the structural nature of the azobenzene alkanethiols on the electrochemical/structural properties of their monolayers at electrode/electrolyte interfaces. Herein, we focus our study on: (a) the dependence of the molecular orientation on the electrode potential, (b) the comparison of molecular packing of monolayers having different alkyl chain lengths, and (c) the relationship between the molecular structure and the electrochemical stability of the azobenzene SAMs. Fourier transform infrared reflection/absorption spectroscopy (FTIR–RAS) coupled with electrochemistry and polarization-modulation, has been progressively introduced into the study of organized monolayers on gold since the 1980s.<sup>21–24</sup> This state-of-the-art technique for probing

\* To whom correspondence should be addressed.

<sup>†</sup> Acadia University.

<sup>‡</sup> Hokkaido University.

(1) Yu, H. Z.; Zhang, H. L.; Liu, Z. F.; Ye, S.; Uosaki, K. *Langmuir* **1998**, *14*, 619.

(2) Wang, R.; Iyoda, T.; Tryk, D. A.; Hashimoto, K.; Fujishima, A. *Langmuir* **1997**, *13*, 4644.

(3) Campbell, D. J.; Herr, B. R.; Hulstee, J. C.; Van Duyne, R. P.; Mirkin, C. A. *J. Am. Chem. Soc.* **1996**, *118*, 10211.

(4) Liu, Z. F.; Hashimoto, K.; Fujishima, A. *Nature* **1990**, *347*, 658.

(5) Ikeda, T.; Sasaki, T.; Ichimura, K. *Nature* **1993**, *361*, 428.

(6) Liu, Z. F.; Morigaki, K.; Hashimoto, K.; Fujishima, A. *Anal. Chem.* **1992**, *64*, 134.

(7) Yu, H. Z.; Wang, Y. Q.; Cheng, J. Z.; Zhao, J. W.; Inokuchi, H.; Fujishima, A.; Liu, Z. F. *J. Electroanal. Chem.* **1995**, *395*, 321.

(8) Yu, H. Z.; Wang, Y. Q.; Cheng, J. Z.; Zhao, J. W.; Inokuchi, H.; Fujishima, A.; Liu, Z. F. *Langmuir* **1996**, *12*, 2843.

(9) Wang, Y. Q.; Yu, H. Z.; Cheng, J. Z.; Zhao, J. W.; Cai, S. M.; Liu, Z. F. *Langmuir* **1996**, *12*, 5466.

(10) Yu, H. Z.; Shao, H. B.; Luo, Y.; Zhang, H. L.; Liu, Z. F. *Langmuir* **1997**, *13*, 5774.

(11) Yu, H. Z.; Wang, Y. Q.; Cai, S. M.; Liu, Z. F. *Ber. Bunsen-Ges. Phys. Chem.* **1997**, *101*, 257.

(12) Herr, B. R.; Mirkin, C. A. *J. Am. Chem. Soc.* **1994**, *116*, 1157.

(13) Caldwell, W. B.; Campbell, D. J.; Chen, K.-M.; Herr, B. R.; Mirkin, C. A.; Malik, A.; Durbin, M. K.; Dutta, P.; Huang, K. G. *J. Am. Chem. Soc.* **1995**, *117*, 6071.

in-situ molecular transformations at electrode/electrolyte interfaces,<sup>25,26</sup> facilitated the accomplishment of our investigations.

## 2. Experimental Section

The azobenzene alkanethiols (CnAzoCmSH) were prepared and purified by published procedures.<sup>1,7–11</sup> The electrolyte was 0.1 M NaClO<sub>4</sub> prepared from Milli-Q water and NaClO<sub>4</sub>·H<sub>2</sub>O (Reagent grade, Wako Pure Chemicals), and was buffered to pH: 5.0 (phosphate buffer).<sup>1</sup> Polycrystalline gold disks (8 mm in diameter and 1 mm thick, 99.98% purity) were used as working electrodes. The surface of the electrode was polished successively with 1.0, 0.3, and 0.05  $\mu$ m alumina on a polishing cloth. The electrode was first cleaned in an ultrasonic bath and then electrochemically by cycling the potential in 0.1 M H<sub>2</sub>SO<sub>4</sub> for 10–20 min prior to surface modification. The electrode was derivatized by immersion in a 0.1 mM ethanol solution of azobenzene alkanethiols (CnAzoCmSH) for 20–24 h. The modified electrode was rinsed with ethanol and Milli-Q water several times before characterization.

FTIR–RAS measurements were carried out using a Bio-Rad, FTS-30 spectrometer with a HgCdTe detector cooled with liquid nitrogen. Nitrogen gas was used to purge atmospheric water and CO<sub>2</sub> in the spectrometer. A homemade IR spectroelectrochemical Teflon cell with a CaF<sub>2</sub> window was used for the in-situ measurements.<sup>1,25</sup> The gold electrode was pressed against the window so that the thickness of the water layer between the window and the electrode surface was minimized. The incidence angle at the electrode surface was  $\sim 65^\circ$  with respect to the surface normal. In-situ spectra of monolayers were obtained as differential spectra between two potentials by employing the method of subtractively normalized interfacial Fourier transform infrared reflection-adsorption spectroscopy (SNIFTIRS).<sup>26</sup> A total of 1024 scans (2 cm<sup>-1</sup> resolution) was recorded for each spectrum with the potential being switched between the reference potential and the sample potential every 64 or 128 scans. The achieved acceptable signal/noise ratios that enabled us to unambiguously determine the peak position as well as to assign the major bands (see Results and Discussion).

Conventional electrochemical measurements were carried out in a standard three-compartment, three-electrode cell. For both electrochemical and spectroelectrochemical studies, a reversible hydrogen electrode (RHE) and a Pt wire were used as reference and counter electrodes, respectively.<sup>1</sup> All the measurements were carried out at room temperature and the electrolyte solution was deoxygenated by bubbling N<sub>2</sub> gas for at least 15 min. All the experiments were repeated more than 3 times and showed very good reproducibility.

## 3. Results and Discussion

### 3.1. Electrochemistry and General Observations.

Figure 1a and 1b show the cyclic voltammograms of AzoC2S–Au monolayers in a conventional electrochemical

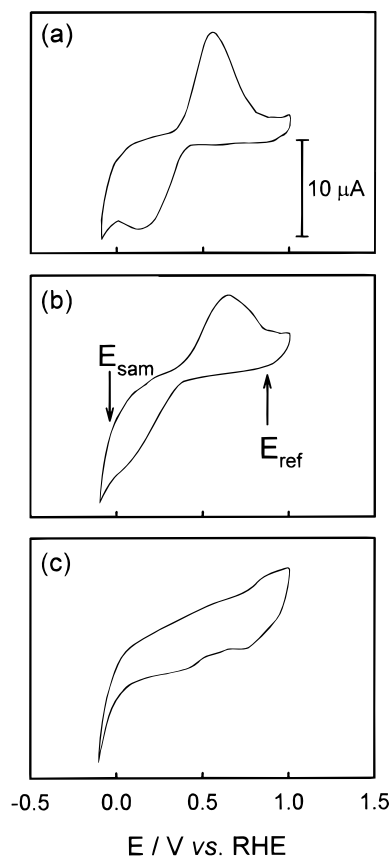


**Figure 1.** Cyclic voltammograms of AzoC2S–Au in 0.1 M NaClO<sub>4</sub>, pH 5.0, phosphate buffer at a scan rate of 0.05 V/s. (a) in a conventional electrochemical cell, (b) in the in-situ FTIR–RAS cell, (c) after the oxidative decomposition experiments (see text for detail).

cell and in the in-situ FTIR cell, respectively. The features in Figure 1a are identical to those reported in our previous paper.<sup>11</sup> The cyclic voltammogram for AzoC2S–Au recorded in the in-situ FTIR cell (Figure 1b) differs from Figure 1a in the peak separation and the area of the redox waves, which is possibly due to distortions induced by the cell geometry. Integration of the area under the voltammetric peaks in Figure 1b, assuming a two-electron reduction/oxidation process, yielded a value equivalent to  $(3.8 \pm 0.4) \times 10^{-10}$  mol/cm<sup>2</sup>. This slightly smaller surface concentration compared to that obtained in a conventional cell with the same modified electrode [ $(4.2 \pm 0.4) \times 10^{-10}$  mol/cm<sup>2</sup>],<sup>11</sup> indicates that a fraction of AzoC2SH molecules adsorbed on the gold surface is isolated electronically from the electrolyte solution, due to the compact touching of the electrode surface to the CaF<sub>2</sub> window.<sup>24</sup> The electrochemical behavior of either C1AzoC2S–Au or C2AzoC4S–Au is similar to that of AzoC2–Au but with a larger peak separation. This was attributed to the slower electron-transfer kinetics in these longer chain azobenzene SAMs, which was explained in terms of longer electron tunneling distance (C2AzoC4S–Au) as well as relatively stronger conformational restriction to the protonation and structural changes.<sup>1,7–11</sup>

In-situ FTIR survey spectra in the range of 3000 cm<sup>-1</sup> to 1150 cm<sup>-1</sup> by using both p- and s-polarization of CnAzoCmS–Au in contact with 0.1 M NaClO<sub>4</sub> at pH 5.0 are shown in Figure 2. As mentioned above, these spectra are differential reflectance spectra obtained at the sample potential ( $E_{\text{sam}}$ ) and the reference potential ( $E_{\text{ref}}$ ), i.e.,  $\Delta R/R = (R_{\text{sam}} - R_{\text{ref}})/R_{\text{sam}}$ , by which potential dependent structural conformation can be evaluated.<sup>21–26</sup> Noting that

(14) Walter, D. G.; Campbell, D. J.; Mirkin, C. A. *J. Phys. Chem. B* **1999**, *103*, 402.

(15) Evans, S. D.; Johnson, S. R.; Ringsdorf, H.; Williams, L. M.; Wolf, H. *Langmuir* **1998**, *14*, 6336.

(16) Wolf, H.; Ringsdorf, H.; Delamarche, E.; Takami, T.; Kang, H.; Michel, B.; Gerber, Ch.; Jaschke, M.; Butt, H.-J.; Bamberg, E. *J. Phys. Chem.* **1995**, *99*, 7107.

(17) Jaschke, M.; Schonherr, H.; Wolf, H.; Butt, H.-J.; Bamberg, E.; Besocke, M. K.; Ringsdorf, H. *J. Phys. Chem.* **1996**, *100*, 2290.

(18) Delamarche, E.; Michel, B. *Thin Solid Films* **1996**, *273*, 54.

(19) Tamada, K.; Nagasawa, J.; Nakanishi, F.; Abe, K.; Ishida, T.; Hara, M.; Knoll, W. *Langmuir* **1998**, *14*, 3264.

(20) Han, S. W.; Kim, C. H.; Hong, S. H.; Chung, Y. K.; Kim, K. *Langmuir* **1999**, *15*, 1579.

(21) Beden, B.; Lamy, C. In *Spectroelectrochemistry: Theory and Practice*; Gale, R. J., Ed.; Plenum Press: New York, 1988; p 189.

(22) Ashley, K.; Pons, B. S. *Chem. Rev.* **1988**, *88*, 673.

(23) Popenoe, D. D.; Deinhammer, R. S.; Porter, M. D. *Langmuir* **1992**, *8*, 2521.

(24) Bae, I. T.; Sandifer, M. S.; Lee, Y. W.; Tryk, D. A.; Sukenik, C. N.; Scherson, D. A. *Anal. Chem.* **1995**, *67*, 4508.

(25) Shimazu, K.; Ye, S.; Sato, Y.; Uosaki, K. *J. Electroanal. Chem.* **1994**, *375*, 409.

(26) Sato, Y.; Ye, S.; Haba, T.; Uosaki, K. *Langmuir* **1996**, *12*, 2726.

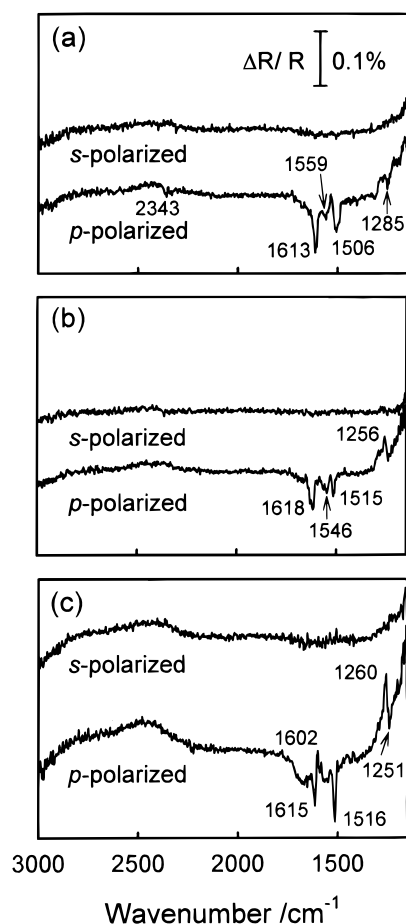


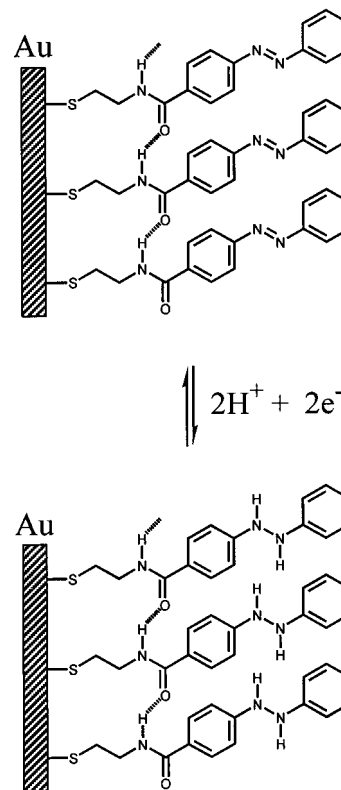
**Figure 2.** Differential survey spectra of (a) AzoC2S-Au, (b) C1AzoC2S-Au, and (c) C2AzoC4S-Au monolayers in 0.1 M NaClO<sub>4</sub>, pH 5.0, phosphate buffer in the 1150 cm<sup>-1</sup> to 3000 cm<sup>-1</sup> region. The spectra were obtained with the reference and sample potential being kept at +0.8 V and -0.1 V (vs RHE), respectively. The collection mode is 8 × 128 scans.

these in-situ FTIR-RAS spectra are reported without baseline correction, and the signal/noise ratios are comparable (AzoC2S-Au and C1AzoC2S-Au) or better (C2AzoC4S-Au) than those reported for SAMs on gold in the literature.<sup>1,2,23-26</sup> For the spectra shown in Figure 2, the reference potential was set at +0.80 V (vs RHE), and the sample potential was chosen to be -0.1 V (vs RHE) (see Figure 1b). All the bands except for the double-peak absorption of atmospheric CO<sub>2</sub> that eventually appears in the spectra at around 2343 cm<sup>-1</sup> (see Figure 2a),<sup>1</sup> can only be observed by using p-polarized light (Figure 2). This suggests that these bands are due to chemisorbed monolayers in accordance with the "surface selection rule" of infrared reflection measurement on metal surfaces.<sup>24</sup> In contrast to the featureless range (3000–2800 cm<sup>-1</sup>) where CH<sub>3</sub> or CH<sub>2</sub> vibrations are expected to show up, several notable bands arise in the region of 1800–1200 cm<sup>-1</sup> as listed in Table 1. Analogous to the electrochemical behavior,<sup>7-14</sup> these spectral features are consistent with the reduction of the surface-confined azobenzene that produces the corresponding hydrazobenzene. The 2H<sup>+</sup>, 2e<sup>-</sup> redox behavior of azobenzene to hydrazobenzene was confirmed and discussed in detail in our previous work,<sup>1</sup> and is also in general agreement with that reported by Wang et al.<sup>2</sup> In brief, the conclusion was drawn based on two major bands appearing in the in-situ spectra. First, the new negative band at 1506–16 cm<sup>-1</sup>, was assigned to the N–H bending mode,<sup>28</sup> showing strong evidence for the production of  $\phi$ -NH–NH– $\phi$  from  $\phi$ -N=N– $\phi$ . Next,

**Table 1. Mode Assignments and Peak Positions (cm<sup>-1</sup>) in the In-Situ FTIR Spectra of C2AzoC4S-Au, C1AzoC2S-Au, and AzoC2S-Au Monolayers**

mode	wavenumber, cm <sup>-1</sup>			direction
	C2AzoC4S-Au	C1AzoC2S-Au	AzoC2S-Au	
benzene ring	1615/1602	1618	1613	bipolar
benzene ring	1587			positive
$\delta_{\text{NH}}$ , $\nu_{\text{CN}}$ (amide II)		1546	1559	negative
$\delta_{\text{NH}}$	1516	1515		negative
benzene ring	1503			positive
$\delta_{\text{NH}}$ , $\nu_{\text{CN}}$ (amide III)			1285	negative
$\nu_a$ ( $\phi$ -O-C)	1260/1251	1256/1247		bipolar

**Scheme 1**



the bipolar peaks at 1613–15/1602 cm<sup>-1</sup>, corresponding to the benzene ring stretching mode, reflect the chemical environmental changes caused by the electroreduction of azobenzene.<sup>29</sup> Scheme 1 presents an illustration of the redox reaction as well as a hypothetical model of the interchain hydrogen bonds in AzoC2S-Au monolayers. The interchain hydrogen bonding is evident as the absence of CH<sub>2</sub>/CH<sub>3</sub> vibration bands (3000–2800 cm<sup>-1</sup>) and C=O stretching band (amide I, ~1640 cm<sup>-1</sup>) in the in-situ FTIR-RAS spectra (Figure 2).<sup>1,11</sup> The existence of interchain hydrogen bonds was also supported by our previous electrochemical stability tests in ethanol.<sup>30</sup> More straightforwardly, our ex-situ grazing angle reflection adsorption IR spectra displayed no C=O (amide I) and N–H stretching bands indicating that these bonds are parallel to the electrode surface as a result of intermolecular hydrogen bonding.<sup>11,30</sup> The above observation of interchain hydrogen bonding in CnAzoCmS-Au SAMs is in excellent agree-

(27) Greenler, R. G. *J. Chem. Phys.* **1966**, *44*, 310.

(28) Hadzi, D.; Skrbliak, M. *J. Chem. Soc. (London)* **1957**, 843.

(29) Pouchert, C. J. *The Aldrich Library of Infrared Spectra*, 3rd ed.; Adrich Co.: Milwaukee, WI, 1981.

(30) Zhang, H. L.; Xia, H.; Li, H. L.; Liu, Z. F. *Chem. Lett.* **1997**, 721.



ment with the grazing-incidence IR studies of other alkanethiol monolayers on gold containing amide linkages.<sup>31–34</sup>

In addition to the common features as mentioned above, the in-situ spectra displayed significant differences between azobenzene SAMs of varying alkyl chain lengths. First, the bipolar bands for  $\nu_{as}(\phi-O-C)$  were not observed because there is no terminal group in AzoC2S–Au. Instead, a negative band generally assigned to the amide III band at  $1285\text{ cm}^{-1}$  was observed in Figure 2a.<sup>35–38</sup> Second, in AzoC2S–Au and C1AzoC2S–Au monolayers, the amide II band at  $1546$  or  $1559\text{ cm}^{-1}$  (Figure 2a and 2b) appeared as negative going, while no such a band was clearly resolved in the in-situ spectrum of C2AzoC4S–Au (Figure 2c). The position of amide II band is important because it gives further insights into the degree of hydrogen bonding among the amide groups. For non-bonded free amide groups, the amide II band will appear at a much lower frequency.<sup>32,34</sup> Since amide II and amide III bands are mixed modes of N–H bending and C–N stretching, the appearance of these bands indicates that structural disorder have occurred when the azobenzene was reduced in these monolayers. The assignment of these amide bands, particularly amide III band, is not conclusive because of the involvement of multiple motions,<sup>38</sup> but it is in good agreement with the ex-situ observation and assignment.<sup>32,34</sup> Third, the band intensities of C2AzoC4S–Au are much stronger and the band shapes are much sharper compared to those of AzoC2S–Au and C1AzoC2S–Au. For instance, the bands corresponding to the benzene ring stretching at  $1587$  and  $1503\text{ cm}^{-1}$  observed in the spectrum of C2AzoC4S–Au are not clearly resolved in the spectra of AzoC2S–Au and C1AzoC2S–Au. This is probably due to the less ordered packing of azobenzene moieties in these SAMs because these vibrational modes all have transition dipole moments parallel to the long axis of azobenzene.<sup>2,39</sup> The direct comparison between the in-situ spectra of CnAzoCmS–Au, indicates a higher degree of molecular organization for the C2AzoC4S–Au monolayer. In other words, the monolayers formed from azobenzene alkanethiols with short alkyl chains are less ordered compared to the monolayers having longer alkyl chains. Therefore, conformational changes in these monolayers are expected to occur during the electrochemical reduction of azobenzene moieties.<sup>2</sup>

Alternatively, the band intensity observed in the in-situ spectra (Figure 2) does not depend on the reaction time, indicating that there is no difference between the rate of reduction for azobenzene and that of oxidation for hydrazobenzene. The facile electron-transfer kinetics in the present systems compared to the unusual slow reduction process reported for the long chain azobenzene

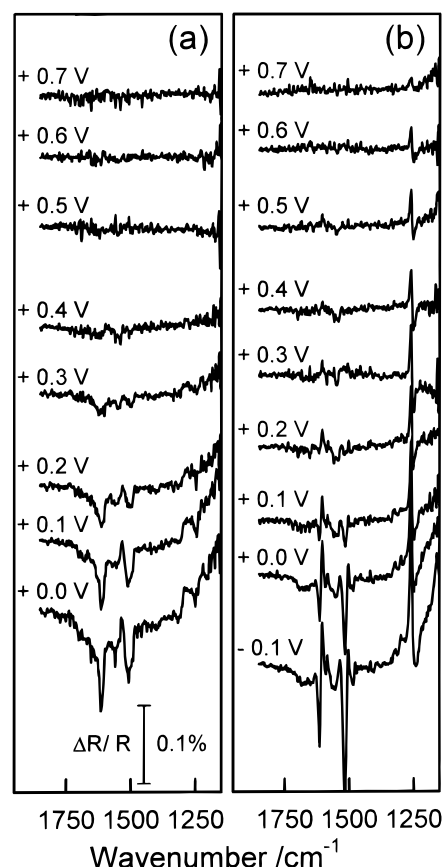


**Figure 3.** Differential spectra of (a) AzoC2S–Au and (b) C2AzoC4S–Au monolayers as a function of the sample potential. The collection mode is  $16 \times 64$  scans, and other conditions are the same as in Figure 2.

SAMs on gold,<sup>1,2</sup> can be understood on the basis of the closer electron tunneling distance (the shorter inner alkyl chains between azobenzene and electrode surface) as well as the weaker structural restriction to the protonation and conformational changes (relatively loosely packed monolayer structures).<sup>7–14</sup> This comparison reinforces the correlation between the length of alkyl chains in the alkanethiols and the overall physical properties of the monolayers as discussed above.

**3.2. Potential Dependent Molecular Orientational Changes.** To further elucidate the possible molecular orientational changes and their structural dependence, a series of differential spectra of AzoC2S–Au and C2AzoC4S–Au monolayers were obtained by varying sample potential  $E_{\text{sam}}$  and setting the reference potential  $E_{\text{ref}}$  constant at  $+0.8\text{ V}$  (Figure 3). The variation of spectral features shown in Figure 3 at each sample potential is reversible. Figure 4 displays the potential dependence of the intensities of typical bands arising in the in-situ spectra of AzoC2S–Au and C2AzoC4S–Au monolayers. The benzene ring stretch ( $1613\text{ cm}^{-1}$ ) and  $\delta_{\text{NH}}$  ( $1506\text{ cm}^{-1}$ ) bands for AzoC2S–Au exponentially decrease when the sample potential shifts to positive direction. When the  $E_{\text{sam}}$  increases to  $+0.4\text{ V}$  (vs RHE), the relative intensities of these two bands drop to zero (Figure 4a), indicating that no reduction of azobenzene occurs in this potential region. The  $\delta_{\text{NH}}$  ( $1516\text{ cm}^{-1}$ ) band of C2AzoC4S–Au also shows similar behavior (Figure 4b), which is in good agreement with the reduction process of azobenzene to hydrazobenzene as discussed above and confirmed in previous studies.<sup>1–3,7–11</sup>

It is striking that the relative intensity of the  $\nu_{as}(\phi-O-C)$  bipolar band ( $1260/1251\text{ cm}^{-1}$ ) of C2AzoC4S–Au

(31) Lenk, T. J.; Hallmark, V. M.; Hoffmann, C. L.; Rabolt, J. F.; Castner, D. G.; Erdelen, C.; Ringsdorf, H. *Langmuir* **1994**, *10*, 4610.

(32) Tam-Chang, S.-W.; Biebuyck, H. A.; Whitesides, G. M.; Jeon, N.; Nuzzo, R. G. *Langmuir* **1995**, *11*, 4371.

(33) Clegg, R. S.; Hutchison, J. E. *Langmuir* **1996**, *12*, 5239.

(34) Zhang, J.; Zhang, H. L.; Chen, M.; Zhao, J.; Liu, Z. F.; Li, H. L. *Ber. Bunsen-Ges. Phys. Chem.* **1998**, *102*, 701.

(35) Silverstein, R. M.; Bassler, G. C.; Morrill, T. C. *Spectrometric Identification of Organic Compounds*, 4th ed.; John Wiley & Sons: New York, 1981.

(36) Miyazawa, T. In *Polyamine Acides*; Fasman, G. D., Ed.; Dekker: New York, 1967.

(37) Lin-Vien, D.; Colthup, N. B.; Fateley, W. G.; Grasselli, J. G. *The Handbook of Infrared and Raman Characteristic Frequencies of Organic Molecules*; Academic Press: New York, 1991.

(38) Bellamy, L. J. *The Infrared Spectra of Complex Molecules*; Chapman and Hall: New York, 1975, Vol. 1, pp 231–262, and references therein.

(39) Nakahara, H.; Fukuda, K. *J. Colloid. Interface Sci.* **1983**, *93*, 530.

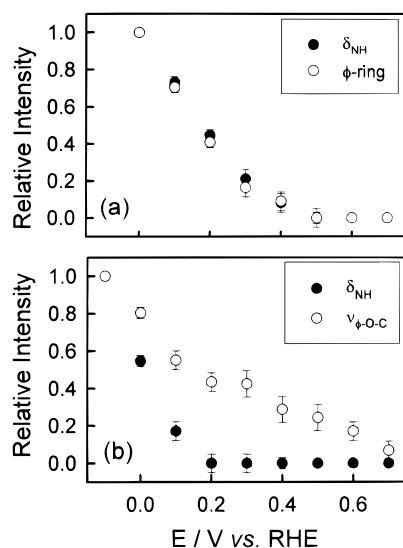
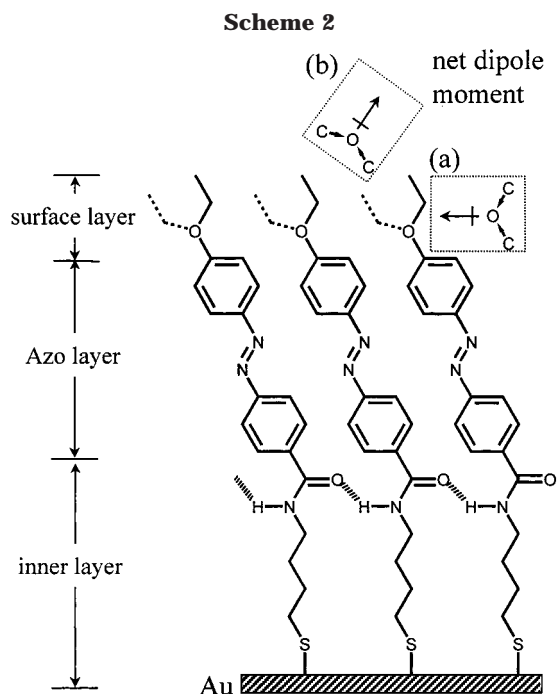


**Figure 4.** The variation of relative intensities of the bands for (a) AzoC2S–Au and (b) C2AzoC4S–Au monolayers (shown in Figure 3) as a function of the sample potential. The band intensities were normalized to (a) 0.0 V and (b) –0.1 V. Experimental uncertainty was determined from the reproducibility of at least three independent measurements.

increases monotonically as the sample potential shifts to negative direction in the whole potential window investigated (+0.7 to –0.1 V vs RHE). In particular, when  $E_{\text{sam}}$  is positive than +0.2 V (vs RHE) where no reduction of azobenzene is expected, the intensity of the  $\nu_{\text{as}}(\phi\text{--O--C})$  bipolar band is likely proportional to the electrode potential change (Figure 4b). The bipolar shape for this band can be understood by the shift of peak position, which is a consequence of the chemical/electrical environmental changes.<sup>1,2</sup> However, the intensity change as a function of potential is normally explained by structural reorientation.<sup>2,26,40</sup> As p-polarized light interacts only with a dipole moment perpendicular to the surface,<sup>21</sup> the nonzero absorption of the  $\nu_{\text{as}}(\phi\text{--O--C})$  band whenever an electrode potential applied (even at where no reduction of azobenzene occurs) means that the terminal ethoxy group reorients closer to the surface normal. In Scheme 2, the two extreme situations for the orientation of the end group are presented. As is shown, the  $\phi\text{--O--C}$  bond angle is about 110°, the dipole moments of the two C–O bonds do not cancel each other; consequently, this group possess a net dipole moment perpendicular to the axis bisecting the C–O–C angle (estimated to be 1.18 D for ethyl ether).<sup>41</sup> Therefore, one of the driving forces for the terminal group reorientation may be the interaction between the dipole moment of the  $\phi\text{--O--C}$  group and the applied electrical field. When the sample potential shifts to a more negative value with respect to the reference potential (+0.80 V vs. RHE), the electric field presumably realigns the molecular dipole according to the direction the electrical field (e.g. switching from a to b as shown in Scheme 2). On the other hand, compared to the giant azobenzene moieties underneath, the ethoxy groups have a greater degree of freedom that allows for a potential-induced reorientation. These results are also complementary to our previous investigations of potential dependent orientational changes in mecaptoalkanenitrile monolayers on gold.<sup>26</sup>

A few aspects of this approach deserve further discussion. First, it could be oversimplified to separate the



potential dependent reorientation from the redox reaction induced reorientation. Wang et al. have concluded that the reduction of azobenzene may be accompanied by an inclination of the terminal azobenzene groups based on the observed decrease in the intensity of the  $\nu_{\text{as}}(\phi\text{--O--C})$  band.<sup>2</sup> Noting that the C–O–C group in their system was positioned underneath the azobenzene moieties, any orientational change of this group has to correlate with the packing of the giant azobenzene groups.<sup>2,42</sup> Second, it is surprising that the dipole moment of the  $\phi\text{--O--C}$  group interacts with the far-distant electrode (~17 Å according to Scheme 2), although the potential dependent orientational changes have been observed for the C≡N group in NC–C<sub>7</sub>H<sub>14</sub>S–Au SAMs (~9 Å).<sup>26</sup> Attention should also be drawn to the fact that no clear potential dependent reorientation of the end group in the long-chain C2AzoC10S–Au SAMs was observed, which could be a reasonable amendment for the distance effect.<sup>1</sup> Third, we have not observed potential dependent reorientation of the terminal group for C1AzoC2S–Au, which can be understood by its relatively disordered structure and lower signal/noise ratio. This may directly relate to the loosely packed azobenzene groups in this monolayer as discussed in the forthcoming sections. Nevertheless, our comprehensive in-situ FTIR–RAS studies enabled us to consider the C2AzoC4S–Au monolayer as a “layer-by-layer” structure as depicted in Scheme 2. It has a unique potential dependent “dynamic” structure: an interchain hydrogen bonded “inner layer”, a redox reaction dominated “Azo layer”, and a potential switchable “surface layer”.

**3.3. Electrochemical Stability of the C<sub>n</sub>AzoC<sub>m</sub>S–Au Monolayers.** The stability of functionalized monolayers is vital for any future applications. Electrochemical desorption methods have been widely used to examine the stability of alkanethiol SAMs on gold both in aqueous and nonaqueous solution over the past decade.<sup>26,43–47</sup> The effect of intermolecular hydrogen bonding in the electro-

(40) Ataka, K.; Yotsuyanagi, T.; Osawa, M. *J. Phys. Chem.* **1996**, *100*, 10664.

(41) Morrison, R. T.; Boyd, R. N. *Organic Chemistry*; Allyn and Bacon Inc.: Needham Heights, NJ, 1976; p 553.

(42) Takeshi, K.; Umemura, J.; Takanaka, T. *Langmuir* **1990**, *6*, 672.

(43) Walczak, M. M.; Popenoe, D. D.; Deinhammer, R. S.; Lamp, B. D.; Chung, C.; Porter, M. D. *Langmuir* **1991**, *7*, 2687.

(44) Widrig, C. A.; Chung, C.; Porter, M. D. *J. Electroanal. Chem.* **1991**, *310*, 335.

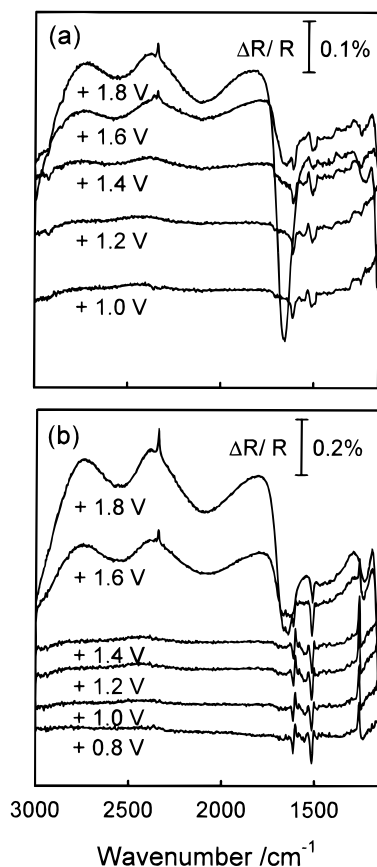


**Figure 5.** Differential spectra of (a) AzoC2S–Au and (b) C2AzoC4S–Au obtained at different positive potentials. The reference potential was adjusted while the sample potential was kept constant at  $-0.1$  V (vs. RHE). Other conditions are the same as in Figure 3.

chemical stability of azobenzene alkanethiol monolayers on gold was preliminarily studied in our previous brief report.<sup>30</sup>

Differential spectra of monolayers of AzoC2S–Au and C2AzoC4S–Au in contact with  $0.1$  M  $\text{NaClO}_4$  at pH 5.0 at different positive potentials (keep  $E_{\text{sam}} = -0.1$  V vs RHE, and shift  $E_{\text{ref}}$ ) are shown in Figure 5. No discernible changes in the spectral feature were observed when the positive potential was below  $+1.2$  V (vs RHE), indicating the azobenzene monolayers are electrochemically stable in this potential region. However, when the potential was higher than  $+1.2$  V, several new bands appeared in addition to those related to the reduction of azobenzene to hydrazobenzene. These spectral changes are irreversible as the intensities of bands related to the reduction of azobenzene decreased with increasing time during which the positive potential was applied. Simultaneously, the intensities of the new bands became much stronger (Figure 5). These results unambiguously show the desorption of azobenzene alkanethiols from gold electrode surfaces when a very positive potential ( $>+1.2$  V vs RHE) was applied. As shown in Figure 1c, the redox waves for azobenzene to hydrazobenzene in the AzoC2S–Au monolayer completely diminished, with considerable enlargement of the double-layer capacitive current, after the in-situ measurements as described in Figure 5.

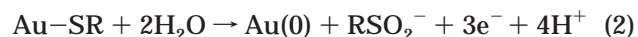
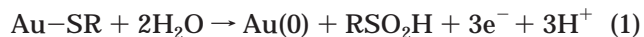
**Table 2. Mode Assignments and Peak Positions ( $\text{cm}^{-1}$ ) of New Bands Appearing in the In-Situ FTIR Spectra of AzoC2S–Au and C2AzoC4S–Au Monolayers with the Sample Potential at  $-0.1$  V and the Reference Potential at  $+1.6$  V (vs RHE)**

mode	wavenumber, $\text{cm}^{-1}$		direction
	C2AzoC4S–Au	AzoC2S–Au	
$\nu_{\text{as}}(\text{CH}_2)$		$\sim 2922$	negative
$\nu_{\text{s}}(\text{CH}_2)$		$\sim 2854$	negative
$\nu(\text{CO}_2)$	2344	2342	positive
$\nu_{\text{as}}(\text{SO}_2)$	$\sim 1310$	$\sim 1312$	positive
$\nu_{\text{s}}(\text{SO}_2)$	1188	1180	positive

The possible assignments and positions of the notable new bands, which arise with shifting the potential to  $+1.6$  V in the region of  $3000$  to  $1150$   $\text{cm}^{-1}$ , are summarized in Table 2. First, the bands around  $2922$  and  $2854$   $\text{cm}^{-1}$  correspond to  $\nu_{\text{as}}(\text{CH}_2)$  and  $\nu_{\text{s}}(\text{CH}_2)$ , respectively. The fact that these bands were not observed when the spectra were acquired in the reversible reduction/oxidation region for azobenzene to hydrazobenzene ( $<+1.2$  V vs RHE), confirms that these bands are from the orientational changes accompanying the decomposition of adsorbed azobenzene alkanethiol molecules.

The sharp peak at  $2342$ – $2344$   $\text{cm}^{-1}$  behaved quite differently from other bands, showing a potential independent peak position while it can be also observed by s-polarized light (not shown in figure). The peak intensity of this band became higher at a more positive potential. As proposed previously,<sup>26</sup> this band is due to  $\text{CO}_2$  in solution generated by anodic oxidation of the adsorbed alkanethiols.

The bands at around  $1310$ – $1312$  and  $1180$ – $1188$   $\text{cm}^{-1}$  are positive and broad. They became stronger when the potential was more positive or was applied for a longer time, suggesting that these bands were generated as a result of irreversible chemical changes of these monolayers. The band positions are in good agreement with those of  $\nu_{\text{as}}(\text{SO}_2)$  and  $\nu_{\text{s}}(\text{SO}_2)$ , which were observed and assigned for SAMs containing sulfones in the ex-situ FTIR studies.<sup>48,49</sup> It is reasonable to attribute these two bands to the sulfone-like groups generated by the oxidation of sulfur–gold bonding. Widrig et al. have proposed possible pathways for the oxidative desorption of the *n*-alkanethiol monolayers from Au/mica electrodes based on the electrochemical measurements:<sup>44</sup>



Pathways 1 and 2 correspond to  $\text{pH} < 4$  and  $\text{pH} > 7$ , respectively. In the present study, the pH was buffered at 5.0, making it difficult to ascertain which route the reaction follows. We believe that the second route is likely favorable, due to the slightly higher wavenumbers of these two bands compared to those reported by Ulman et al.<sup>48</sup>

It is important to compare the electrochemical stability of SAMs on gold formed from azobenzene alkanethiols of different alkyl chain lengths. As shown in Figure 5b, the bands corresponding to  $\nu_{\text{as}}(\text{CH}_2)$  and  $\nu_{\text{s}}(\text{CH}_2)$ , were not clearly observed even with an applied potential up to  $+1.8$  V (vs RHE) for C2AzoC4S–Au. This indicates that the C2AzoC4S–Au monolayer is more stable upon oxidative

(45) Schneider, T. W.; Buttry, D. A. *J. Am. Chem. Soc.* **1993**, *115*, 12391.

(46) Everett, W. R.; Welch, T. L.; Reed, L.; Fritsch-Faules, I. *Anal. Chem.* **1995**, *67*, 292.

(47) Beulen, M. W. J.; Kastenbergh, M. I.; van Veggel, F. C. J. M.; Reinhoudt, D. N. *Langmuir* **1998**, *14*, 7463.

(48) Evans, S. D.; Urankar, E.; Ulman, A.; Ferris, N. *J. Am. Chem. Soc.* **1991**, *113*, 4121.

(49) Ulman, A.; Evans, S. D.; Snyder, R. G. *Thin Solid Films* **1992**, *210/211*, 806.



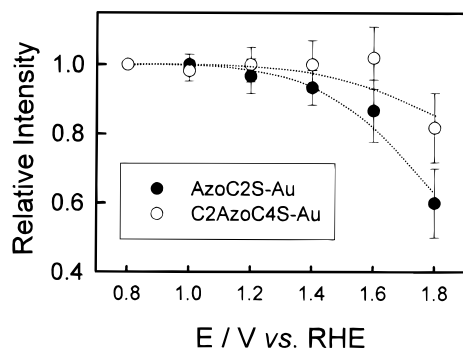


**Figure 6.** The variation of relative intensity of the  $\delta_{\text{NH}}$  band of (a) AzoC2S-Au and (b) C2AzoC4S-Au monolayers (shown in Figure 5) as a function of the electrode potential. The band intensities were normalized to (a) +1.0 V and (b) +0.8 V. The dotted lines are to direct eyes only.

decomposition compared to its shorter chain counterpart (AzoC2S-Au).<sup>50</sup> In both monolayers, no clear evidence has been observed for the decomposition of azobenzene moieties (up to +1.6 V vs RHE), indicating that azobenzene groups are more resistant to oxidation compared to reductive decomposition which was discussed in our previous paper.<sup>8</sup>

To have a clear comparison of the stability of different azobenzene monolayers, Figure 6 plots the relative intensities of the  $\delta_{\text{NH}}$  band of C2AzoC4S-Au and AzoC2S-Au as a function of the applied positive potential. The diminishing rates of the redox band ( $\delta_{\text{NH}}$ ) are significantly different from each other in these two monolayers, providing direct evidence for the different stability derived from alkanethiol molecules having varied alkyl chains. Higher electrochemical stability is expected with longer alkyl chain lengths in the molecule. For example, at +1.8 V (vs RHE), the loss of AzoC2S-Au monolayer is more than 40%, but for C2AzoC4S-Au it is only ~15%. The better electrochemical stability of C2AzoC4S-Au can be understood as a result of better organization and a more closely packed monolayer structure. The hydrophobic character of oriented alkyl chains can effectively protect Au-S bonds from attack by electrolyte molecules. The blocking of electrolyte molecules or ions penetrating into

the highly oriented azobenzene SAMs was also evident from previous electrochemical measurements.<sup>7-14</sup>

#### 4. Conclusion

An extended electrochemical in-situ FTIR-RAS study of azobenzene SAMs at gold/aqueous electrolyte interfaces has been performed in order to give insights into the molecular orientation and electrochemical stability of these monolayers. The in-situ spectroscopic results provide strong evidence for the potential dependence of a "layered" structure of azobenzene SAMs on gold (Cn-AzoCmS-Au): hydrogen bonding fixed "inner layer" (the alkyl chain between azobenzene and electrode surface), redox active "Azo layer", and orientational switchable "surface layer" (the terminal group). The irreversible anodic decomposition of the monolayers was studied to elucidate the electrochemical stability of azobenzene SAMs. The destruction of these monolayers produces new features in the in-situ spectra related to the  $\text{CH}_2$  vibrations and the oxidative products ( $\text{CO}_2$  and alkyl sulfonates). A possible reaction pathway to form  $\text{R-SO}_2^-$  was suggested. More importantly, for the first time, the in-situ FTIR-RAS technique was applied to demonstrate the correlation between alkyl chain length and the overall physical properties of the monolayer, including the molecular order, the redox behavior, and the chemical stability. It has been shown that with either a longer alkyl chain in between the functional moiety and electrode surface or a longer terminal group exposed to the electrolyte, better packed and oriented monolayers with higher stability were obtained. Efforts made to address this issue will impact on the further molecular design and construction of organized molecular systems.

**Acknowledgment.** We acknowledge the financial support from the Ministry of Science and Technology, the Ministry of Education, and the National Natural Science Foundation of China. This work was also supported by grants-in-aid for Scientific Research from the Ministry of Education, Science, Sports, and Culture, Japan. It is a pleasure to draw attention to the fact that the work described in the present paper, as has so much other research on functional azobenzene monolayers, benefited significantly from the stimulating ideas and experimental innovations which have emanated from Professor Akira Fujishima and his research group. H.Z.Y. thanks Professor Katsumi Niki and Professor Akira Fujishima for their support for his stay in Japan, and also thanks Drs. Louis Cuccia, James Wojtyk, and Sarah Anderson (NRC Canada) for their reviewing of the manuscript.

LA000054M

(50) The reorientation of alkyl chains is expected after partially oxidative decomposition of C2AzoC4S-Au SAMs. No clear  $\nu_{\text{as}}(\text{CH}_2)$  and  $\nu_{\text{s}}(\text{CH}_2)$  bands were observed even at +1.8 V (vs RHE) probably due to the ratio of decomposition being quite small, or the reaction product ( $\text{R-SO}_2^-$ ) remaining on the electrode surface. Further studies will involve  $\text{R-SO}_2\text{H}$  monolayers on gold to clarify this point as well as to further confirm the oxidative decomposition pathway.